Asymptotic Error Bounds on Prediction of Narrowband MIMO Wireless Channels

Ramoni O. Adeogun, *Student Member, IEEE,* Pawel A. Dmochowski, *Senior Member, IEEE,* and Paul D. Teal, *Senior Member, IEEE*

***Abstract*—In this letter, we derive simple expressions for the lower bound on the prediction error variance for narrowband MIMO channel with uniform linear array at both ends of the link. The derived bounds show the relationship between the achievable prediction performance and prediction algorithm design parameters, thereby providing useful insights into the development of fading channel prediction algorithms.**

***Index Terms*—Channel prediction, parameter estimation, Cramer Rao bound, MIMO, multipath fading**

I. Introduction

CHANNEL state prediction has been well addressed in the literature for link adaptation in MIMO systems (see e.g., [1–4]). However, to the authors' knowledge, there exist no closed form expression that relates CSI prediction error to predictor design parameters such as number of antennas, number of samples in the observation segment, number of paths and SNR. In [5, 6], bounds on the prediction error in SISO channels were derived. The authors of [7] derived an asymptotic error bound on the prediction of SISO OFDM channels. Bounds on the prediction of narrowband MIMO channels were studied in [8].

Although, the bound derived in [8] is useful in its own way, it requires averaging over several realizations of the channel in order to obtain results that are independent of the actual channel parameters. Moreover, its expression is not readily interpretable.

Motivated by the need for simple, insightful and easily interpretable closed form expressions relating prediction error to algorithm design parameters, and the benefits of having bounds upon which the performance of any predictor can be compared, we make the following contributions in this paper:

- Using the vector formulation of the Cramer Rao bound for functions of parameters [9] along with the properties of Kronecker products, we derive expressions for bounds on the prediction of MIMO channels with uniform linear arrays (ULA) at both ends of the link. The formulations obtained are simpler and provide an alternative for easier calculation compared to the results of [8].
- We derive a simple closed–form expression for the best achievable mean square error (MSE) and normalized mean square error (NMSE) for an unbiased joint estimator and predictor in the asymptotic limit of large samples and/or many antenna elements. The derived expression provides useful insights into the development of algorithms for MIMO channel prediction.
- Simulation results show that the asymptotic bound offers a very good approximation to the bound while eliminating the need for repeated computation and dependence on channel parameters.

Copyright (c) 2012 IEEE. Personal use of this material is permitted. However, permission to use this material for any other purposes must be obtained from the IEEE by sending a request to pubs-permissions@ieee.org.

The authors are with the School of Engineering and Computer Science, Victoria University of Wellington, New Zealand (E-mail: [ramoni.adeogun, paul.teal, pawel.dmochowski]@ecs.vuw.ac.nz)

II. Channel Models

We consider the ray–based channel model defined for a MIMO channel at the zth sampling interval as

$$\mathbf{H}(z) = \sum_{p=1}^{P} \alpha_{\mathrm{p}} \mathbf{a}_{\mathrm{r}}(\mu_p^{\mathrm{r}}) \mathbf{a}_{\mathrm{t}}^T(\mu_p^{\mathrm{t}}) e^{jz\nu_p} \tag{1}$$

where $[\cdot]^T$ denotes the transpose operation. P is the number of paths, and α_p and ν_p are the complex amplitude and normalized radian Doppler frequency of the pth path. The receive and transmit array response vectors associated with the pth path are denoted by $\mathbf{a}_{\mathrm{r}}(\mu_p^{\mathrm{r}})$ and $\mathbf{a}_{\mathrm{t}}(\mu_p^{\mathrm{t}})$, respectively, where μ_p^{r} and μ_p^{t} are the angular frequencies associated with the directions of arrival and departure of the pth path, respectively. Note that while (1) is valid for all antenna geometries, we will consider a ULA such that $\mathbf{a}_{\mathrm{r}}(\mu_p^{\mathrm{r}})$ is defined by

$$\mathbf{a}_{\mathrm{r}}(\mu_p^{\mathrm{r}}) = [1 \quad e^{-j\mu_p^{\mathrm{r}}} \quad e^{-j2\mu_p^{\mathrm{r}}} \quad \cdots \quad e^{-j(N-1)\mu_p^{\mathrm{r}}}]^T \tag{2}$$

where $\mu_p^{\mathrm{r}} = 2\pi\delta_{\mathrm{r}} \sin\theta_p$. N is the number of receive antenna elements, δ_{r} is the inter element spacing of the receive array and θ_p is the angle of arrival of the pth path. The transmit array response vector is analogously defined by replacing N with M and μ_p^{r} with μ_p^{t}. A useful representation for our derivations is the vectorized version of the channel matrices defined as

$$\mathbf{h}(z) = \sum_{p=1}^{P} \alpha_p (\mathbf{a}_{\mathrm{r}}(\mu_p^{\mathrm{r}}) \otimes \mathbf{a}_{\mathrm{t}}(\mu_p^{\mathrm{t}})) e^{jz\nu_p} \tag{3}$$

where $\otimes$ denotes the Kronecker product. We assume that, for the purpose of channel prediction, Z samples of the channel are known either from channel estimation or measurement. In practice, the channel estimates contain some amount of error, $\mathbf{w}(z)$ resulting from noise and interference. The estimated channel can therefore be modelled as

$$\hat{\mathbf{h}}(z) = \mathbf{h}(z) + \mathbf{w}(z); \quad z = 0, 1, \cdots, Z-1 \tag{4}$$

For convenience, the Z measured samples can be collected into an $NMZ \times 1$ vector $\hat{\mathbf{h}} = [\hat{\mathbf{h}}^T(1) \quad \cdots \quad \hat{\mathbf{h}}^T(Z)]^T$ which can be shown using (3) to be

$$\hat{\mathbf{h}} = \sum_{p=1}^{P} \alpha_p(\mathbf{a}_{\mathrm{r}}(\mu_p^{\mathrm{r}}) \otimes \mathbf{a}_{\mathrm{t}}(\mu_p^{\mathrm{t}}) \otimes \mathbf{a}_{\mathrm{d}}(\nu_p)) + \mathbf{w} \tag{5}$$

where $\mathbf{a}_{\mathrm{d}}(\nu_p) = [1 \quad e^{j\nu_p} \quad e^{j2\nu_p} \quad \cdots \quad e^{j(Z-1)\nu_p}]^T$. A matrix representation of (5) is thus

$$\begin{aligned}\hat{\mathbf{h}} &= \left(\mathbf{A}_{\mathrm{r}}(\boldsymbol{\mu}^{\mathrm{r}}) \diamond \mathbf{A}_{\mathrm{t}}(\boldsymbol{\mu}^{\mathrm{t}}) \diamond \mathbf{A}_{\mathrm{d}}(\boldsymbol{\nu})\right)\boldsymbol{\alpha} + \mathbf{w} \\ &= \mathbf{A}\boldsymbol{\alpha} + \mathbf{w}\end{aligned} \tag{6}$$

where $\diamond$ denotes the Khatri-Rao product, $\boldsymbol{\alpha} = [\alpha_1 \quad \cdots \quad \alpha_P]^T$ and $\mathbf{A}_{\mathrm{r}}(\boldsymbol{\mu}^{\mathrm{r}})$ is the Vandermonde structured steering matrix defined as

$$\mathbf{A}_{\mathrm{r}}(\boldsymbol{\mu}^{\mathrm{r}}) = [\mathbf{a}_{\mathrm{r}}(\mu_1^{\mathrm{r}}) \quad \mathbf{a}_{\mathrm{r}}(\mu_2^{\mathrm{r}}) \quad \cdots \mathbf{a}_{\mathrm{r}}(\mu_P^{\mathrm{r}})] \tag{7}$$

$\mathbf{A}_{\mathrm{t}}(\boldsymbol{\mu}^{\mathrm{t}})$ and $\mathbf{A}_{\mathrm{d}}(\boldsymbol{\nu})$ are defined analogously.

III. Prediction Error Bound

In this section, we derive the lower bound on the prediction MSE for narrowband channels. Although a similar error bound has been derived in [8], we utilize the properties of Khatri-Rao product to present an alternative, simplified derivations and expression for the Fisher information matrix (FIM). Let the parametrization of the channel be represented by

$$\boldsymbol{\Theta} = \begin{bmatrix}\Re(\boldsymbol{\alpha}) & \Im(\boldsymbol{\alpha}) & \boldsymbol{\mu}^{\mathrm{r}} & \boldsymbol{\mu}^{\mathrm{t}} & \boldsymbol{\nu}\end{bmatrix} \tag{8}$$

where $\boldsymbol{\mu}^{\mathrm{r}} = [\mu_1^{\mathrm{r}} \quad \cdots \quad \mu_P^{\mathrm{r}}]$, $\boldsymbol{\mu}^{\mathrm{t}} = [\mu_1^{\mathrm{t}} \quad \cdots \quad \mu_P^{\mathrm{t}}]$ and $\boldsymbol{\nu} = [\nu_1 \quad \cdots \quad \nu_P]$. $\Re[\cdot]$ and $\Im[\cdot]$ denote the real and imaginary parts of the associated complex number, respectively. An alternative formulation which we do not present here has the Doppler frequencies dependent on the angles of arrival. The results are not significantly different from those presented here except in the case that the angle between the array and direction of travel approaches zero. To emphasize dependence on channel parameters, (6) can now be written as

$$\hat{\mathbf{h}} = \mathbf{A}(\boldsymbol{\Theta})\boldsymbol{\alpha} + \mathbf{w} \tag{9}$$

Assuming that $\mathbf{w} \sim \mathcal{CN}(0, \sigma^2\mathbf{I})$, the measured data is distributed as $\hat{\mathbf{h}} \sim \mathcal{CN}(\boldsymbol{\mu}_{\mathrm{h}}, \sigma^2\mathbf{I})$, with $\boldsymbol{\mu}_{\mathrm{h}} = \mathbf{A}(\boldsymbol{\Theta})\boldsymbol{\alpha}$. Since the channel represents a non-linear function of its parameters, the bound on prediction error can be found using [9]

$$\mathrm{MSEB}(z) = \mathrm{Tr}\left[\frac{\partial\hat{\mathbf{h}}(z,\boldsymbol{\Theta})}{\partial\boldsymbol{\Theta}}^H \mathbf{I}^{-1}(\boldsymbol{\Theta})\frac{\partial\hat{\mathbf{h}}(z,\boldsymbol{\Theta})}{\partial\boldsymbol{\Theta}}\right] \tag{10}$$

where $\mathrm{Tr}[\cdot]$ denotes the sum of the diagonal elements of the associated matrix. $\mathrm{MSEB}(z) = \mathrm{Tr}\left[\mathbb{E}[(\hat{\mathbf{h}}(z) - \mathbf{h}(z))(\hat{\mathbf{h}}(z) - \mathbf{h}(z))^H]\right]$, $\mathbf{I}^{-1}(\boldsymbol{\Theta})$ is the CRLB on multiple parameter estimation, $\mathbf{I}(\boldsymbol{\Theta})$ is the FIM and the Jacobian in (10) is defined by

$$\frac{\partial\hat{\mathbf{h}}(z)}{\partial\boldsymbol{\Theta}} = \left[\frac{\partial\hat{\mathbf{h}}(z)}{\partial\Re(\boldsymbol{\alpha})} \quad \frac{\partial\hat{\mathbf{h}}(z)}{\partial\Im(\boldsymbol{\alpha})} \quad \frac{\partial\hat{\mathbf{h}}(z)}{\partial\boldsymbol{\mu}^{\mathrm{r}}} \quad \frac{\partial\hat{\mathbf{h}}(z)}{\partial\boldsymbol{\mu}^{\mathrm{t}}} \quad \frac{\partial\hat{\mathbf{h}}(z)}{\partial\boldsymbol{\nu}}\right] \tag{11}$$

Using Bangs formula [9], entries of the FIM can be evaluated using

$$[\mathbf{I}(\boldsymbol{\Theta})]_{ij} = \mathrm{Tr}\left[\mathbf{C}^{-1}\frac{\partial\mathbf{C}}{\partial\boldsymbol{\Theta}_i}\mathbf{C}^{-1}\frac{\partial\mathbf{C}}{\partial\boldsymbol{\Theta}_j}\right] + 2\Re\left[\frac{\partial\mathbf{h}^H}{\partial\boldsymbol{\Theta}_i}\mathbf{C}^{-1}\frac{\partial\mathbf{h}}{\partial\boldsymbol{\Theta}_j}\right] \tag{12}$$

where $\mathbf{C} = \sigma^2\mathbf{I}$ is the noise covariance matrix. Since the covariance matrix is not dependent on the parameters, only the second term of (12) is non-zero and (12) reduces to

$$\mathbf{I}(\boldsymbol{\Theta}) = \frac{2}{\sigma^2}\Re\left[\frac{\partial\mathbf{h}}{\partial\boldsymbol{\Theta}}^H\frac{\partial\mathbf{h}}{\partial\boldsymbol{\Theta}}\right] \tag{13}$$

The first order derivative with respect to each of the parameter vector are evaluated as follows

$$\begin{aligned}\frac{\partial\mathbf{h}}{\partial\boldsymbol{\theta}} &= (\mathbf{D}_{\mathrm{r}} \diamond \mathbf{A}_{\mathrm{t}} \diamond \mathbf{A}_{\mathrm{d}})\mathbf{X} \qquad \frac{\partial\mathbf{h}}{\partial\boldsymbol{\phi}} = (\mathbf{A}_{\mathrm{r}} \diamond \mathbf{D}_{\mathrm{t}} \diamond \mathbf{A}_{\mathrm{d}})\mathbf{X} \\ \frac{\partial\mathbf{h}}{\partial\boldsymbol{\nu}} &= (\mathbf{A}_{\mathrm{r}} \diamond \mathbf{A}_{\mathrm{t}} \diamond \mathbf{D}_{\mathrm{d}})\mathbf{X} \quad \frac{\partial\mathbf{h}}{\partial\Re(\boldsymbol{\alpha})} = (\mathbf{A}_{\mathrm{r}} \diamond \mathbf{A}_{\mathrm{t}} \diamond \mathbf{A}_{\mathrm{d}}) \\ \frac{\partial\mathbf{h}}{\partial\Im(\boldsymbol{\alpha})} &= j\,(\mathbf{A}_{\mathrm{r}} \diamond \mathbf{A}_{\mathrm{t}} \diamond \mathbf{A}_{\mathrm{d}})\end{aligned} \tag{14}$$

where $\mathbf{X} = \mathrm{diag}[\boldsymbol{\alpha}]$ and $\mathbf{D}_{\mathrm{r}}$ is defined for the ULA as

$$\mathbf{D}_{\mathrm{r}} = \left[\frac{\partial\mathbf{a}_{\mathrm{r}}(\theta_1)}{\partial\theta_1} \quad \cdots \frac{\partial\mathbf{a}_{\mathrm{r}}(\theta_P)}{\partial\theta_P}\right] = -j\mathbf{F}_N\mathbf{A}_{\mathrm{r}} \tag{15}$$

where $\mathbf{F}_k$ is a diagonal matrix defined by

$$\mathbf{F}_k = \mathrm{diag}[0 \quad 1 \quad \cdots \quad k-1] \tag{16}$$

$\mathbf{D}_{\mathrm{t}}$ and $\mathbf{D}_{\mathrm{d}}$ are defined analogously. Using (14), the Jacobian in (13) can now be expressed as

$$\begin{aligned}\frac{\partial\mathbf{h}}{\partial\boldsymbol{\Theta}} = [&\mathbf{A}_{\mathrm{t}} \diamond \mathbf{A}_{\mathrm{d}} \diamond \mathbf{D}_{\mathrm{r}}\mathbf{X} \quad \mathbf{A}_{\mathrm{r}} \diamond \mathbf{D}_{\mathrm{t}} \diamond \mathbf{A}_{\mathrm{d}}\mathbf{X} \\ &\mathbf{A}_{\mathrm{r}} \diamond \mathbf{A}_{\mathrm{t}} \diamond \mathbf{D}_{\mathrm{d}}\mathbf{X} \quad \mathbf{A} \quad j\mathbf{A}]\end{aligned} \tag{17}$$

which, using the properties of Khatri-Rao and Kronecker products can be expressed as

$$\frac{\partial\mathbf{h}}{\partial\boldsymbol{\Theta}} = \mathbf{P}_4 \diamond \mathbf{P}_3 \diamond \mathbf{P}_2 \diamond \mathbf{P}_1 \tag{18}$$

where

$$\mathbf{P}_1 = \begin{bmatrix}\boldsymbol{\alpha}^T & \boldsymbol{\alpha}^T & \boldsymbol{\alpha}^T & \mathbf{1}^1 & j\mathbf{1}^T\end{bmatrix} \tag{19}$$

$$\mathbf{P}_2 = [\mathbf{D}_{\mathrm{r}} \quad \mathbf{A}_{\mathrm{r}} \quad \mathbf{A}_{\mathrm{r}} \quad \mathbf{A}_{\mathrm{r}} \quad \mathbf{A}_{\mathrm{r}}] \tag{20}$$

$$\mathbf{P}_3 = [\mathbf{A}_{\mathrm{t}} \quad \mathbf{D}_{\mathrm{t}} \quad \mathbf{A}_{\mathrm{t}} \quad \mathbf{A}_{\mathrm{t}} \quad \mathbf{A}_{\mathrm{t}}] \tag{21}$$

$$\mathbf{P}_4 = [\mathbf{A}_{\mathrm{d}} \quad \mathbf{A}_{\mathrm{d}} \quad \mathbf{D}_{\mathrm{d}} \quad \mathbf{A}_{\mathrm{d}} \quad \mathbf{A}_{\mathrm{d}}] \tag{22}$$

The Fisher information matrix is thus

$$\mathbf{I}(\boldsymbol{\Theta}) = \frac{2}{\sigma^2}\Re\left[(\mathbf{P}_4 \diamond \mathbf{P}_3 \diamond \mathbf{P}_2 \diamond \mathbf{P}_1)(\mathbf{P}_4 \diamond \mathbf{P}_3 \diamond \mathbf{P}_2 \diamond \mathbf{P}_1)^H\right] \tag{23}$$

Using the following property of Khatri-Rao product

$$(\mathbf{A} \diamond \mathbf{B})^H(\mathbf{A} \diamond \mathbf{B}) = (\mathbf{A}^H\mathbf{A}) \odot (\mathbf{B}^H\mathbf{B}) \tag{24}$$

where $\odot$ denotes element-wise multiplication, (23) can be written as

$$\mathbf{I}(\boldsymbol{\Theta}) = \frac{2}{\sigma^2}\Re\left[(\mathbf{P}_4^H\mathbf{P}_4) \odot (\mathbf{P}_3^H\mathbf{P}_3) \odot (\mathbf{P}_2^H\mathbf{P}_2) \odot (\mathbf{P}_1^H\mathbf{P}_1)\right] \tag{25}$$

Finally, using (25) and (10), the prediction MSEB can be computed.

IV. Asymptotic Error Bound

As shown in Section III, the bound on the prediction error can be found using (10). However, it is not readily interpretable and its dependence on the actual channel parameters necessitates numerical averaging for specified probability distributions. The computational load becomes significant for large values of N, M, and Z. In this section, we derive simple and easily interpretable closed–from expressions for the lower bound on the prediction MSE and NMSE. Using (1), entries of the MIMO channel matrix can be expressed as

$$h(n,m,z)=\sum_{p=1}^{P}\alpha_p e^{j(z\nu_p-(n-1)\mu_p^{\mathrm{r}}-(m-1)\mu_p^{\mathrm{t}})} \tag{26}$$

for all $n=1,\cdots,N$, $m=1,\cdots,M$ and $z=0,\cdots,Z-1$. The channel is re-parametrized as

$$\boldsymbol{\Theta}=\left[\boldsymbol{\theta}_1^T,\cdots,\boldsymbol{\theta}_P^T\right] \tag{27}$$

where

$$\boldsymbol{\theta}_p=[\Re(\alpha_p)\quad \Im(\alpha_p)\quad \mu_p^{\mathrm{r}}\quad \mu_p^{\mathrm{t}}\quad \nu_p]^T \tag{28}$$

Assuming that the error is Gaussian with variance σ^2, entries of the FIM can be computed using

$$[\mathbf{I}(\boldsymbol{\theta})]_{ij}=\frac{2}{\sigma^2}\Re\left(\sum_{z=0}^{Z-1}\sum_{n=1}^{N}\sum_{m=1}^{M}\frac{\partial h}{\partial\theta_i}\frac{\partial h}{\partial\theta_j}^H\right) \tag{29}$$

where the partial derivatives with respect to each parameter can be shown following straightforward derivations as

$$\frac{\partial h}{\partial\Re(\alpha_p)}=e^{j(z\nu_p-(n-1)\mu_p^{\mathrm{r}}-(m-1)\mu_p^{\mathrm{t}})} \tag{30}$$

$$\frac{\partial h}{\partial\Im(\alpha_p)}=je^{j(z\nu_p-(n-1)\mu_p^{\mathrm{r}}-(m-1)\mu_p^{\mathrm{t}})} \tag{31}$$

$$\frac{\partial h}{\partial\mu_p^{\mathrm{r}}}=-j(n-1)\alpha_p e^{j(z\nu_p-(n-1)\mu_p^{\mathrm{r}}-(m-1)\mu_p^{\mathrm{t}})} \tag{32}$$

$$\frac{\partial h}{\partial\mu_p^{\mathrm{t}}}=-j(m-1)\alpha_p e^{j(z\nu_p-(n-1)\mu_p^{\mathrm{r}}-(m-1)\mu_p^{\mathrm{t}})} \tag{33}$$

$$\frac{\partial h}{\partial\nu_p}=jz\alpha_p e^{j(z\nu_p-(n-1)\mu_p^{\mathrm{r}}-(m-1)\mu_p^{\mathrm{t}})} \tag{34}$$

Using (29) and (30) – (34), and performing some simplifications, the FIM submatrix corresponding to the pth path is obtained as

$$[\mathbf{I}(\boldsymbol{\theta}_p)]=\frac{NMZ}{\sigma^2}\begin{bmatrix}2&0&0&0&0\\0&2&0&0&0\\0&0&\frac{2N^2}{3}&\frac{NM}{2}&-\frac{NZ}{2}\\0&0&\frac{NM}{2}&\frac{2M^2}{3}&-\frac{MZ}{2}\\0&0&-\frac{NZ}{2}&-\frac{MZ}{2}&\frac{2Z^2}{3}\end{bmatrix} \tag{35}$$

where we have assumed that Z, N and/or M are large[1]. Note that under this assumption, parameter identifiability which results in rank-deficient FIM in SISO channels is not a problem [8]. We also assumed that the complex amplitude is Gaussian distributed ($\alpha_p\sim\mathcal{CN}(0,1)$) such that $\mathbb{E}[|\alpha_p|^2]=1$ and $\mathbb{E}[\Re(\alpha_p)]=\mathbb{E}[\Im(\alpha_p)]=0$. Assuming that the scattering sources are uncorrelated, the FIM has a block diagonal structure

$$[\mathbf{I}(\boldsymbol{\Theta})]=\mathrm{blkdiag}[\mathbf{I}(\boldsymbol{\theta}_1)\quad \mathbf{I}(\boldsymbol{\theta}_2)\quad \cdots\quad \mathbf{I}(\boldsymbol{\theta}_P)] \tag{36}$$

Using the structure of (36), the inverse can be obtained by inverting each submatrix, that is

$$[\mathbf{I}(\boldsymbol{\theta}_p)]^{-1}=\frac{\sigma^2}{NMZ}\begin{bmatrix}\frac{1}{2}&0&0&0&0\\0&\frac{1}{2}&0&0&0\\0&0&\frac{21}{5N^2}&-\frac{9}{5MN}&\frac{9}{5ZN}\\0&0&-\frac{9}{5MN}&\frac{21}{5M^2}&\frac{9}{5ZM}\\0&0&\frac{9}{5ZN}&\frac{9}{5ZM}&\frac{21}{5Z^2}\end{bmatrix} \tag{37}$$

The variance of the parameter estimates are therefore bounded by the diagonal entries of (37). Using the CRB for functions of parameters, the asymptotic MSEB (AMSEB) is

$$\mathrm{AMSEB}(z)=\frac{1}{NM}\sum_{n=1}^{N}\sum_{m=1}^{M}\frac{\partial h(n,m,z)}{\partial\boldsymbol{\Theta}}[\mathbf{I}(\boldsymbol{\Theta})]^{-1}\frac{\partial h(n,m,z)}{\partial\boldsymbol{\Theta}}^H \tag{38}$$

Due to the diagonal structure of the FIM and independence of FIM submatrices on path parameters, the AMSEB can be written as

$$\mathrm{AMSEB}(z)=\frac{P}{NM}\sum_{n=1}^{N}\sum_{m=1}^{M}\frac{\partial h(n,m,z)}{\partial\boldsymbol{\theta}}[\mathbf{I}(\boldsymbol{\theta})]^{-1}\frac{\partial h(n,m,z)}{\partial\boldsymbol{\theta}}^H \tag{39}$$

Note that for the same signal-to-noise ratio (SNR), the noise variance for a P path channel is $\sigma_P^2=P\sigma^2$, where σ^2 is the noise variance for a single path channel at the same SNR. Using (37) and (39), and after some simplifications, the asymptotic MSEB is obtained as

$$\mathrm{AMSEB}(z)=\frac{P^2\sigma^2}{5NMZ}\left(\frac{29}{2}-\frac{18z}{Z}+\frac{21z^2}{Z^2}\right) \tag{40}$$

for $z=0,1,2,\cdots$, where $z\in(0,Z-1)$ corresponds to the estimation/measurement segment and prediction starts at $z=Z$. In this form, (40) provide useful insights into the effects of the number of antennas, the number of paths, SNR and the number of samples on the MSEB. The first constant term is the contribution from time independent parameters (i.e., amplitude, AOA and AOD) and their cross terms, the second term results from the cross terms involving the Doppler frequency and the third, quadratic term is the contribution from the Doppler frequency estimation. This emphasises the need for accurate estimation of the Doppler frequencies.

V. Numerical Simulations

In this section, we study the effects of various parameters on the error bounds and compare the bound with the asymptotic bound. For our simulations, we utilized the normalized MSEB (NMSEB) defined as $\mathrm{NMSEB}=\mathrm{MSEB}/P$. The NMSE bound is averaged over 500 independent realizations of the channel. The channel parameters are generated for each realization as follows. The complex amplitudes are randomly drawn from a complex Gaussian distribution as

[1]A necessary assumption is that NMZ is large, such that the approximation $\sum_{i=1}^{NMZ}a\approx NMZ\mathbb{E}[a]$ holds.

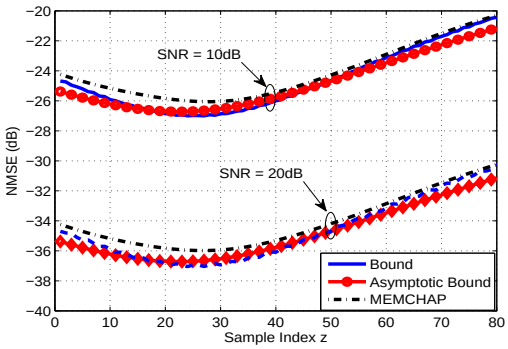

Fig. 1: NMSEB versus sample index with $Z = 50$, $N = 2$ and $M = 2$. MEMCHAP is the ESPRIT based algorithm proposed in [10].

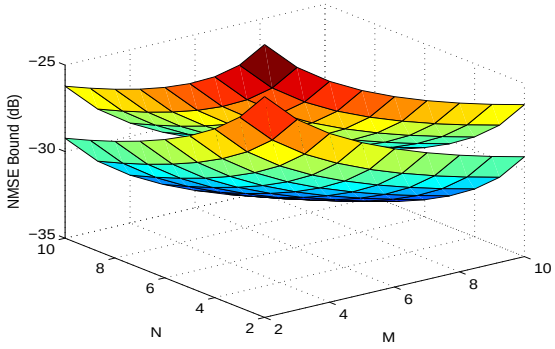

Fig. 3: NMSEB versus number of antennas for a prediction horizon of 10 sampling intervals with $Z = 50$ and $P = 5$.

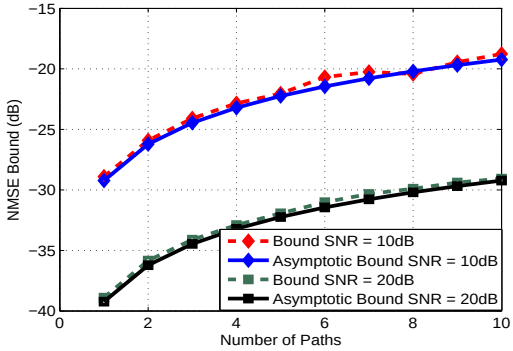

Fig. 2: NMSEB versus number of paths for a prediction horizon of 10 sampling intervals.

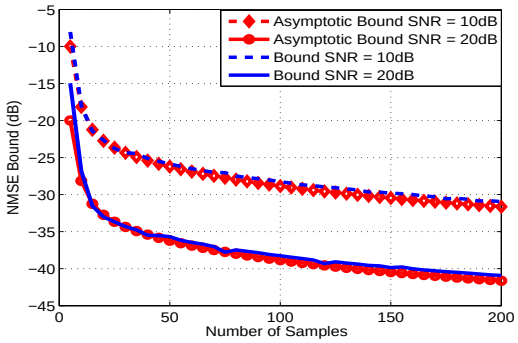

Fig. 4: NMSEB versus number of samples in the measurement segment.

$\alpha_p \sim \mathcal{CN}(0,1)$. The angles of arrival and departure are both selected from a uniform distribution as $\theta_p^{\mathrm{r}}, \theta_p^{\mathrm{t}} \sim \mathcal{U}[-\pi, \pi)$. The Doppler frequencies are generated from a spatial rather than temporal point of view as $\nu_p = 2\pi\Delta x \sin\theta_p^{\mathrm{v}}$, where Δx is the spatial sampling interval in wavelengths and θ_p^{v} is the angle between the direction of travel of the mobile station and the receive antenna array. We also select θ_p^{v} from a uniform distribution as $\theta_p^{\mathrm{v}} \sim \mathcal{U}[-\pi, \pi)$. For our simulations, we consider a sampling interval of 10 samples per wavelength.

Fig. 1 presents the NMSE bounds for a two path channel with $Z = 50$, $N = 2$ and $M = 2$ versus estimated and predicted sample index and compares these with the performance of the multidimensional ESPRIT based prediction scheme (MEMCHAP) in [10]. With the sampling interval used for the NMSE bound computation and MEMCHAP prediction, this corresponds to a measurement length of 5λ and prediction segment of 3λ. As seen from the figure, the NMSE bounds increase quadratically with increasing prediction horizon. In Fig. 2, we plot the NMSE bounds versus the number of paths for a prediction horizon of 10 samples ($1\,\lambda$). We observed that the NMSE bounds increases with increasing number of paths. This agrees with previous observations that propagation channels having dense multipath are more difficult to predict [5, 8]. Fig. 3 shows the effect of the number of antenna at the transmit and receive ends of the MIMO link on the prediction NMSE bound using the asymptotic error bound. As can be seen, the NMSE decreases with increasing number of antennas at either or both ends. We plot the NMSE bound versus the number of samples in the observation segment for a 2×2 channel with $P = 2$ in Fig. 4. We observe that the NMSE decreases with increasing number of samples. This is intuitively satisfying since increased number of samples leads to improved parameter estimation and hence, better prediction. Using a criterion similar to that in [8], a predicted sample is useful if $\mathrm{NMSE} \leq 0.05$ ($\approx$ -13 dB).

VI. Conclusion

In this contribution, we derived simple and easily interpretable closed form expressions for the lower bound on prediction error in MIMO channels with ULA at both ends of the link. The expressions provide useful insights into the effects of parameters such as number of antennas, number of training samples, noise level and number of paths on the prediction error and are independent of the actual channel parameters. Simulation results show that the asymptotic error bound provide a good approximation to the NMSE bound. Future work will derive similar expression for other array geometries.

REFERENCES

[1] J. Vanderpypen and L. Schumacher, "MIMO Channel Prediction using ESPRIT based Techniques," in *Proc. International Symposium on Personal, Indoor and Mobile Radio Communications*, 2007, pp. 1–5.

[2] R. O. Adeogun, P. D. Teal, and P. A. Dmochowski, "Parametric Channel Prediction for Narrowband Mobile MIMO Systems Using Spatio-Temporal Correlation Analysis," in *Proc. IEEE Vehicular Technology Conference Fall*, Sep 2013.

[3] K. Okino, T. Nakayama, S. Joko, Y. Kusano, and S. Kimura, "Direction based beamspace MIMO channel prediction with ray cancelling," in *Proc. International Symposium on Personal, Indoor and Mobile Radio Communications*, 2008, pp. 1–5.

[4] K. E. Baddour, C. C. Squires, and T. J. Willink, "Mobile Channel Prediction with Application to Transmitter Antenna Selection for Alamouti Systems," in *Proc. IEEE Vehicular Technology Conference Fall*, 2006, pp. 1–6.

[5] P. Teal and R. Vaughan, "Simulation and performance bounds for real-time prediction of the mobile multipath channel," in *Proc. IEEE Workshop on Statistical Signal Processing Proceedings*, 2001, pp. 548–551.

[6] S. Barbarossa and A. Scaglione, "Theoretical bounds on the estimation and prediction of multipath time-varying channels," in *Proc. IEEE International Conference on Acoustics, Speech, and Signal Processing*, vol. 5, 2000, pp. 2545–2548 vol.5.

[7] I. C. Wong and B. L. Evans, "Sinusoidal Modeling and Adaptive Channel Prediction in Mobile OFDM Systems," *IEEE Trans. on Sig. Proc.*, vol. 56, no. 4, pp. 1601–1615, 2008.

[8] T. Svantesson and A. Swindlehurst, "A performance bound for prediction of MIMO channels," *IEEE Trans. Sig. Proc.*, vol. 54, no. 2, pp. 520–529, Oct 2006.

[9] S. M. Kay, *Fundamentals of statistical signal processing: estimation theory*. Upper Saddle River, NJ, USA: Prentice-Hall, Inc., 1993.

[10] R. O. Adeogun, P. A. Dmochowski, and P. D. Teal, "Long range parametric channel prediction for narrowband MIMO systems with joint parameter estimation," in *Proc. Seventh International Conference on Signal Processing and Communication Systems*, Dec 2013, pp. 575–580.